ATLANTIS PRESS
Advances in Engineering Research (AER), volume 135
2nd International Conference on Civil, Transportation and Environmental Engineering (ICCTE 2017)

Effect of ZnO/Tourmaline on Inhibition of SRB: A Theoretical Account

Meng Gong
North China Electric Power University, Beijing 102206, P. R. China
dele333@126.com

Keywords: Sulfate Reducing Bacteria (SRB); ZnO/Tourmaline ;Density Functional Theory (DFT)
Abstract. Potential mechanism of inhibition of Sulfate Reducing Bacteria (SRB) at the presence of ZnO/Tourmaline was further investigated by Density Functional Theory (DFT) calculation. The structure and electronic states analysis quantitatively and qualitatively dictate the selectively catalytic generation of OH and OOH on different ZnO surface. Results confirms that $OH^{-0.57}$ on ZnO(101) and $OOH^{-0.27}$ on ZnO(100) is chemically active, which should act as ROS for the inhibition of SRB. Tourmaline showed synergetic effect on the accumulation of H_2O on ZnO surface, which will favor the generation reaction of reactive oxygen species (ROS), hence promoting the inhibition of SRB.

Introduction

Sulfate reducing bacteria (SRB) use sulfate or other oxide sulfur compound as oxidizing agent, reducing to sulfide. SRB belong to 9 bacterial phyla and over 200 species [1]. SRB are the main reason to cause the microbiologically influenced corrosion by accelerating corrosion rate, inducing stress corrosion and pitting corrosion [2,3]. According to statistics of Petrochina in 1997, the financial loss due to corrosion was amount to 0.25 billion Yuan. The sterilization and inhibition of SRB is the main concern in oil field.Many biological approaches to SRB inhibition were employed in previous researches. SO_4^{2-} reduction was inhibited by addition of NO^{3-} in anoxic paddy soil. Nitrate reducers, and sulfate reducers compet for electron donors [4]. NO^{2-}, denitrification products NO and N_2O were more competent for inhibition of bacteria than nitrate [5]. These methods is aimed to control sulfide emission rely on increasing redox potential. However, all of these methods have a problem with the high cost.Addition of oxidizing chemicals such as H_2O_2 or chlorines chemically oxidizes sulfide, thereby decreasing the amount of dissolved sulfide [6]. Cerium-doped TiO_2 film with bactericidal activity was prepared on 304 stainless steel by a sol-gel process [7]. The intrinsic mechanism of inhibiting SNB is not investigated so far.

Herein, the potential mechanism of inhibition of SRB at the presence of the prepared nano ZnO/Turmaline was theoretically investigated using Density Functional Theory (DFT) calculations. H_2O interacts to different site of ZnO related to different reaction paths resulting in the generation of different surface species was discussed and confirmed weather they are ROS for the inhibition of SRB. The synergetic effect of Turnaline for the ZnO/Turmaline in the aqueous solution system was detected. Such fundamental understanding of the synergetic effect of Turnaline and the selective catalytic generation of ROS on different ZnO surfaces will contribute to the design and development of high-performance bacterial inhibitors for environmental science, biological sciences, medicine and materials science.

Meterisl and Method

In reference to the catalytic reaction based on supported cluster models[8,9], DFT and periodic slab models were used to study the interaction between H_2O on ZnO surface. All calculations were performed using DFT with the generalized gradient approximation (GGA) and PBE method to realize the exchange correlation energy of the system. All reactants, products, and intermediates were completely optimized. Optimization of the energy, displacement and force convergence were used as a criterion. Convergence valve were 1.0×10^{-5} eV/atom, 5.0×10^{-3} Å and 4.0×10^{-3} eV/Å respectively.

A complete linear synchronous transit (LST) and quadratic synchronous (QST) search algorithm was employed to identify the transition state of this dissociation reaction and the transition state that had a unique imaginary frequency[10].

Molecular dynamics (MD) simulation procedures were used to investigate the adsorption of H_2O on ZnO surface. In the MD simulation, the conjugate gradient method is used for the minimization. The self-adsorption of H_2O onto ZnO surface was minimized under the conditions of constant pressure and constant temperature (NPT) ensembles[11]. The simulation protocol, with the time step of 1 fs to integrate Newton's equation of motion and the saving frequency of every 10 ps for the coordinates of the structures, helps to ensure the stability of the simulation process. Nonbonded cut-off of 15.5 Å was applied to truncate the long-range interaction to speed up the computation. The particle-mesh Ewald method (PME) algorithm with cubic-spline interpolation (1 Å grid width) was applied to calculate electrostatic interactions efficiently[12].

Results and discussion

Potential mechanism of inhibition of SRB

As reported, Zn2+ liberation and reactive oxygen species (ROS) production are thought to be the two potential toxic mechanisms of ZnO, and it is generally accepted that ROS is a major factor in the inhibition of bacteria[13]. However, it is lack of qualitative and quantitative research on the type and activity of ROS. Herein, the investigation begins with the interaction between different surfaces of ZnO under hypoxic environment.

Figure 1 shows the stable structures and the related calculated potential energy profiles for the adasorption of H_2O on ZnO. The interactions initiate from the optimized physisorption configuration, and then the final state relates to the dissociated adsorption of H_2O on ZnO. Results of Figure 1a suggests that H_2O chemically interacts to the bridge site between the Zn atom and O atom of ZnO(100) surface, leading to the generation of OH group and H atom, and H_2O acts as electron accepter in the adsorption system.

Figure 1b illustrates the adsorption of H_2O on the bridge site between two O atoms of ZnO(100) surface from the physisorption state to the final state, which is exothermic, and the reaction energy is -3.868 eV. At the physisorption state (reactant) there is no electron transfer and repopulation between H2O and ZnO(100) according to the calculation of charge population. However with H2O's approaching to ZnO(100), OOH group and OH group generated at the intermediate state. The charge population on OOH group and OH group is -0.520 and -0.590, respectively. Then with further electronic interaction happen between ZnO(100) and OOH group and OH group, the intermediate changed into the product, which the charge population on OOH group and OH group is -0.270 and 0.600, respectively. Comparing Figure 1a with Figure 1b, we can observe that H_2O interacts to different site of ZnO(100) related to different reaction paths resulting in the generation of different surface species.

Figure 1c depicts the stable adsorption configuration of H_2O on the long bridge site between Zn atom and O atom of ZnO(101) surface from the physisorption state through the intermediate state to the product. This process has to climb over a small energy barrier of about 0.004 eV at the intermedicate state and then goes into the final state with the release of 0.743 eV.

Further, we definitively identified the adsorbed species by analyzing the structure and electronic states. The bond length of the generated OH groups shown in Figure 1a, b, and c, is 0.947 Å, 0.944 Å, and 0.946 Å, respectively, which are shorter than that of the pure hydroxyl radical (0.961 Å) and the hydroxyl ion (0.951 Å). The total charge for the generated OH groups shown in Figure 1a, b, and c, is, -0.57, and -0.57, respectively, which transfer from ZnO surface making the spin zero. These generated OH groups shown in Figure 1a, b, and c can be denoted as $OH^{-0.60}$, $OH^{-0.57}$, and $OH^{-0.57}$, respectively. We further analyzed the density of state (DOS) and orbit of the generated $OH^{-0.60}$, OH-0.57, $OH^{-0.57}$, $OOH^{-0.27}$. Figure 2 depicts the DOS, integrated DOS, highest occupied molecular orbit (HOMO) and lowest unoccupied molecular orbit (LUMO) of ·OH, OH^-, and the generated OH group on ZnO(100)

and ZnO(101), b) DOS and integrated DOS of H_2O_2, and the generated OOH group on ZnO(100). The DOS of OH^- located at around -4.5 eV and -0.5 eV with two large peaks. The DOS of ·OH delocalizes at the range of -4.5 eV to -2.5 eV, and the range of -1.0 eV to 0.5 eV. According to the peack around Fermi energy (0.0 eV), the outer molecular orbit of ·OH is half filled, corresponding to the integrated DOS of ·OH (9 atoms) and OH^- (10 atoms), respectively. The delocalization and the half fill of ·OH contributed to the high reaction activity. The DOS of $OH^{-0.60}$ shown in Figure 1a move to lower energy while compared to that of ·OH and OH-, which would be less chemically active. The DOS of $OH^{-0.57}$ shown in Figure 1c is delocalized and half-filled at around Fermi energy, which is very similar to the DOS of ·OH. Therefore the $OH^{-0.57}$ shown in Figure 1c would be high chemically active as ·OH for inhibition of SRB. DOS of $OOH^{-0.27}$, while compared to that of H_2O_2, delocalized from -15.0 V to -11.0 eV and from -3.0 eV to 0.5 eV, the outer bonding-orbit of which is all half-filled. This property will make $OOH^{-0.27}$ as reactive oxygen species.

2p-orbit of O atom contributes to the HOMO of ·OH and OH^-, respectively. However, while anti-bonding orbital (4σ*) of OH^- contributes to the LUMO, the unfilled 2p-orbit of O atom contributes to the HOMO of ·OH. For $OH^{-0.60}$ shown in Figure 1a, 2p-orbit of O atom contributes to the HOMO and 2p-orbit of O atom together with part of O-H bond contributes to the LUMO. For $OH^{-0.57}$ and $OOH^{-0.27}$ shown in Figure 1b, 2p-orbit of O atom contributes to the HOMO of $OH^{-0.57}$and the anti-bonding orbital contributes to the LUMO of $OH^{-0.57}$, 2p-orbits of the two O atoms contribute to both HOMO and LUMO of $OOH^{-0.27}$, which corresponds to the half-filled DOS and the spin analysis.

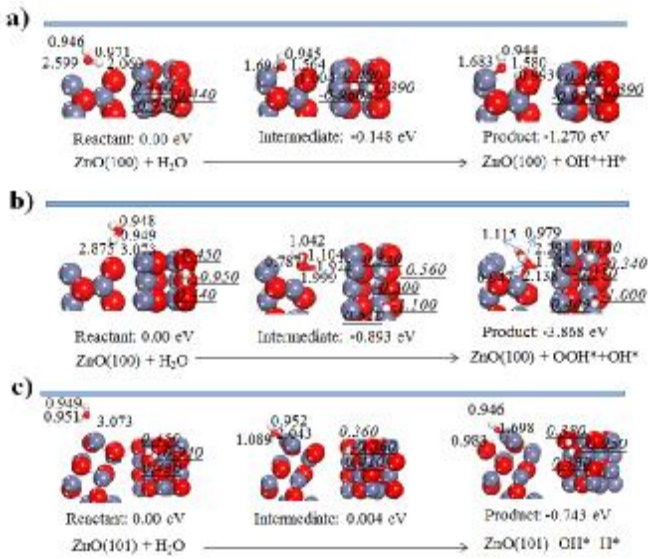

Figure 1 Structures and the related calculated potential energy profiles for the adsorption of water molecule on ZnO. Distances are given in units of Å. Charges of the atoms are underlined.

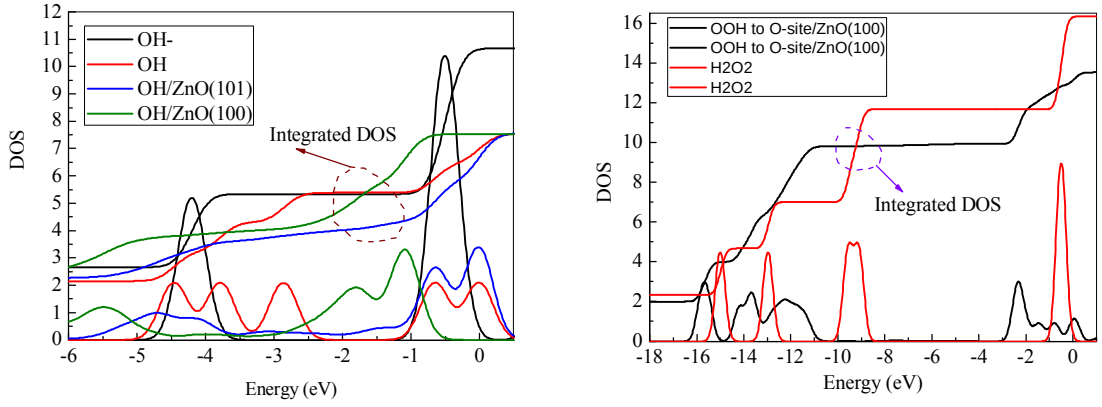

Figure 2 a) DOS and integrated DOS of ·OH, OH^-, $OH^{-0.60}$, $OH^{-0.57}$, and $OH^{-0.57}$. b) DOS and integrated DOS of H_2O_2, and $OOH^{-0.27}$.

Synergetic effect of Tourmaline on ZnO

Figure 3 lists the density field for H_2O over ZnO. The red output field represents a small density distribution of H_2O over ZnO(100) and ZnO(100)/Turnaline lattice framework while the blue output field represents a high density distribution of H_2O over ZnO(100) and ZnO(100)/Turnaline lattice framework. That more H_2O molecules are adsorbed more closely to surface of ZnO(100)/Turnaline than to the surface of ZnO(100), implying a certain synergetic effect of Turnaline for the adsorption H_2O to ZnO surface.

The adsorption isotherms of H_2O on ZnO at room temperature are shown in Figure 3b, which displays the adsorption of H_2O molecules per nm2 at each fugacity. The total fugacity reports the sum of the sorbate component fugacities in kPa. That the adsorption isotherms of H_2O belong to Langmuir-type; i.e., the adsorption capacities initially increase quickly and almost reach the maximum value at around 2000 kPa. In Figure 3, the adsorption capacity and the slope of the adsorption curve before reaching the maximum adsorption capacity for ZnO(100)/Turnaline is large than those for ZnO(100), suggesting that Turnaline favour the adsorption of H_2O on ZnO surface.

The adsorption energy distribution for individual isotherms can be further calculated from the general adsorption integral equation, given by:

$$\Gamma_t(p,T) = \int \Gamma(p,T,U) f(U) dU \tag{4}$$

where Γt denotes the overall adsorption isotherm, Γ the local adsorption isotherm on surface having an interaction energy U, and f(U) is the energy distribution function to be obtained [37].

According to the adsorption isotherm of H_2O on ZnO above, the local adsorption isotherm models Langmuir [38] can be applied. While the maximum adsorption potential energy for the adsorption on ZnO(100)/Turnaline is located around -0.54 eV, the maximum adsorption potential energy for the adsorption on ZnO(100) is at around -0.48 eV (Figure 3 black line). Such effect is possibly related to the synergetic effect of Turnaline, which can usually promote the accumulation of H_2O on the surface of ZnO, hence favoring the generation of ROS to inhibit SRB.

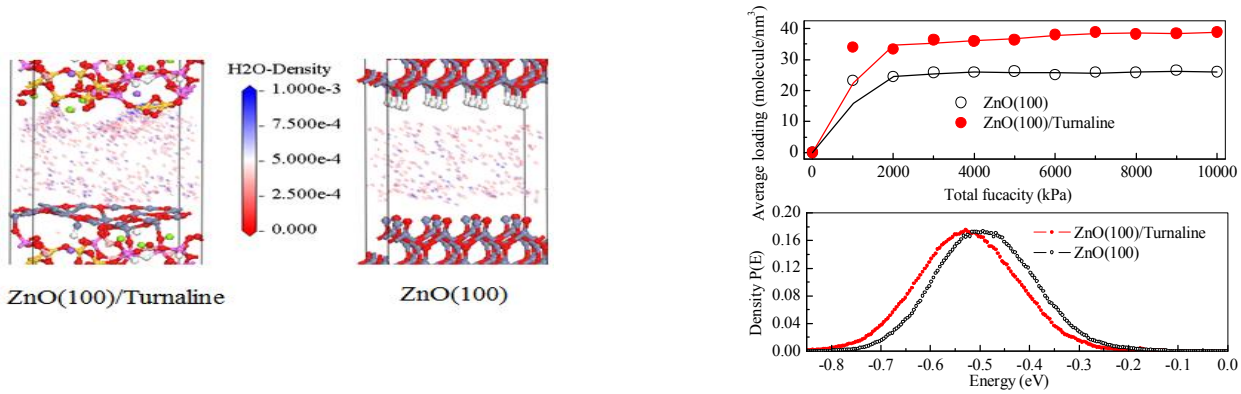

Figure 3 Density field for H_2O over ZnO, b) adsorption isotherms and energy distribution functions P(E) of H_2O over ZnO atom room temperature

Conclusions

The potential mechanism of inhibition of SRB at the presence of ZnO/Turmaline were investigated qualitatively and quantitatively research using DFT calculations. H_2O interacts to different site of ZnO related to different reaction paths resulting in the generation of different surface species. The generated OH groups and OOH group on ZnO surfaces can be denoted as $OH^{-0.60}$, $OH^{-0.57}$, $OH^{-0.57}$, and $OOH^{-0.27}$, respectively. We further analyzed the density of state (DOS) and orbit of the generated $OH^{-0.60}$, $OH^{-0.57}$, $OH^{-0.57}$, $OOH^{-0.27}$. The structure and electronic states analysis quantitatively and qualitatively dictate the selectively catalytic generation of OH and OOH on different ZnO surface. Results confirms that $OH^{-0.57}$ on ZnO(101) and $OOH^{-0.27}$ on ZnO(100) is chemically active, which should as ROS for the inhibition of SRB. Further Turnaline promotes the interaction and accumulation of H_2O on the surface

of ZnO, hence favoring the generation of ROS to inhibit SRB. Fundamental understanding of the synergetic effect of Turnaline and the selective catalytic generation of ROS on different ZnO surfaces will contribute to the design and development of high-performance bacterial inhibitors for environmental science, biological sciences, medicine and materials science.

Acknowledgement

The authors wish to thank the Fundamental Research Funds for the 111 Project (B12034).

References

[1] D. Starosvetsky, J. Starosvetsky, R. Armon, Y. Ein-Eli. A peculiar cathodic process during iron and steel corrosion in sulfate reducing bacteria (SRB) media[J]. Corrosion Science, 2010,52:1536~1540

[2] [3] Sadegh Sh. Abedi, Ail .Abdolmaleki, N. Adibi, Failure analysis of SCC and SRB induced cracking of a transmission oil products pipeline. Engineering Failure Analysis, vol. 14, pp 250-261, 2007.

[4] Achtnich C, Bak F, Conrad R. Competition for electron donors among nitrate reducers, ferric iron reducers, sulfate reducers, and methanogens in anoxic paddy soil. Biol Fertility Soils 1995;19:65-72.

[5] Zumft W G. The biological role of nitric oxide in bacteria[J]. Arch. Microbiol., 1993,160:253-264.

[6] Setareh M, Javaherdashti R. Assessment and control of MIC in a sugar cane factory[J] .Materials and Corrosion, 2003, 54: 259~263.

[7] Hongfen Wang, Zhiqi Wang Haixia Hong Yansheng Yin. Preparation of cerium-doped TiO2 film on 304 stainless steel and its bactericidal effect in the presence of sulfate-reducing bacteria (SRB) [J]Materials Chemistry and Physics,2010,124 :791~794

[8] W.Qin, X. Li, Phys. J. Chem. C 114 (2010) 19009.

[9] W. Qin, X. Li, J. Chem. Phys. Lett. 502 (2011) 96.

[10] Y. Li, L. Tang, J. Li, Electrochem. Commun. 11 (2009) 846.

[11] J.C. Phillips, R. Braun, W. Wang, J. Gumbart, E. Tajkhorshid, E. Villa, C. Chipot, R. D. Skeel, L. Kale, K. Schulten. J. Comput. Chem. 26 (2005) 1781.

[12] T. Darden, D. York, L. Pedersen. J. Chem. Phys. 98 (1993) 10089.

[13] X. R. Liu, J. H. Li, Y. Zhang, Y. S. Ge, F. F. Tian, J. Dai, F. L. Jiang and Y. Liu, J. Membr. Biol., 2011, 244, 105–112